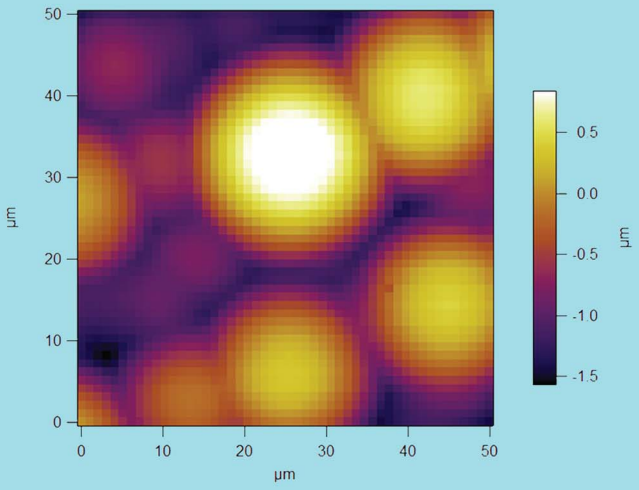

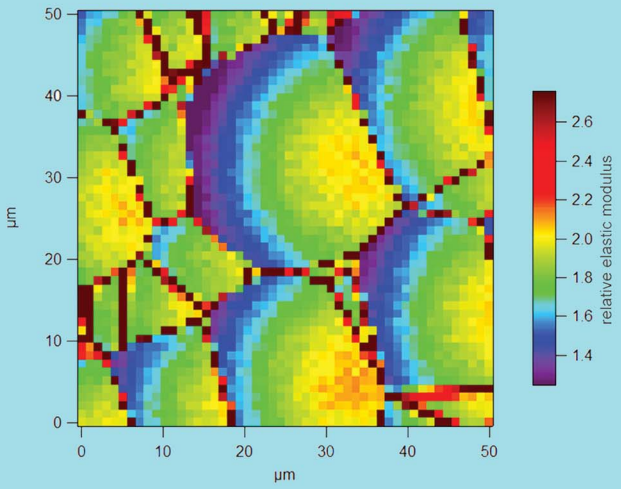

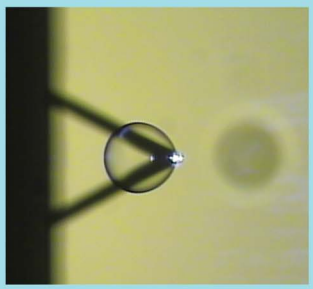

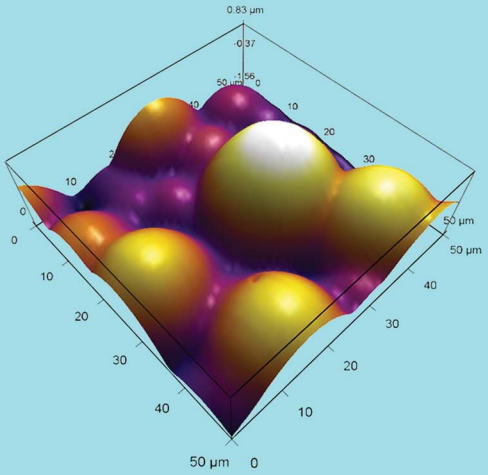

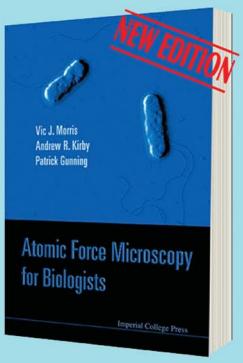

IFR
Institute of
Food Research

Showcasing research from 'Food & Health', a BBSRC collaborative research programme at the Institute of Food Research.

Title: Probing the role of interfacial rheology in the relaxation behaviour between deformable oil droplets using force spectroscopy

AFM images of oil droplets obtained by force mapping reveal both their shape and relative elasticity. A more subtle factor which controls stability of the dispersed phase in emulsions is the role of interfacial composition in determining thin film drainage rates. The paper demonstrates how this can be established by pressing lever-bound oil droplets against sessile oil droplets under water.

As featured in:

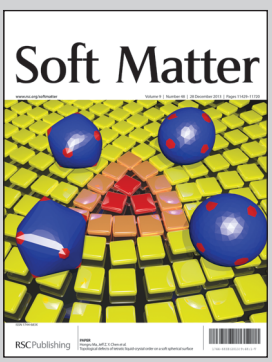

See A. Patrick Gunning *et al.*, *Soft Matter*, 2013, **9**, 11473.

RSC Publishing

www.rsc.org/softmatter

Registered Charity Number 207890

Soft Matter

RSC Publishing

PAPER

View Article Online
View Journal | View Issue

Cite this: *Soft Matter*, 2013, **9**, 11473

Probing the role of interfacial rheology in the relaxation behaviour between deformable oil droplets using force spectroscopy

A. Patrick Gunning,* Andrew R. Kirby, Peter J. Wilde, Robert Penfold, Nicola C. Woodward and Victor J. Morris

Received 4th September 2013
Accepted 15th October 2013

DOI: 10.1039/c3sm52341a

www.rsc.org/softmatter

An experimental method is presented for investigating the effect of the nature of the interface on the relaxation behaviour accompanying hydrodynamic drainage occurring between oil droplets driven together in aqueous solution. This method is based upon force spectroscopy of droplet–droplet interactions. An atomic force microscope is used to drive two droplets together to a pre-defined force and then monitor relaxation of the force between the droplets. It is suggested that the observed relaxation is controlled by the hydrodynamic drainage of the interlamellar fluid separating the droplets. Data is presented for both ionic (sodium dodecyl sulphate) and non-ionic surfactants (Tween-20), uncoated oil droplets and droplets coated with the proteins, β-casein and β-lactoglobulin. Uncoated droplets, droplets coated with surfactants and droplets coated with the protein β-casein all exhibited fast relaxation, whereas droplets coated with β-lactoglobulin exhibited markedly slower relaxation and more complex behaviour.

Introduction

A common feature of many disperse systems is the thin liquid film (TLF) that structurally defines distinct but closely neighbouring bulk phases. Foams comprise a TLF separating cells of vapour while colloidal suspensions, sols and pastes exhibit a TLF between solid solutes. An immiscible TLF demarcating liquid phases constitutes an emulsion. Hybrid situations are also ubiquitous where a TLF forms a membrane or coating among gases, liquids and solids. Important chemical engineering applications include froth floatation and liquid–liquid extraction, but TLFs are also prominent in otherwise disparate phenomena ranging from geology (*e.g.* lava flows) to biophysics (*e.g.* lung linings, tear films, lipid digestion). As models for emulsion stability against coalescence, TLFs are particularly relevant in the design of pharmaceutical delivery vehicles and processed food products. Both microscopic[1,2] and macroscopic[3] TLFs have been thoroughly reviewed.

The presence of interfacially active components strongly influences the dynamics of TLFs, especially in emulsion systems. It has previously been demonstrated that the deformability of oil droplets in water is sensitive to the mechanical characteristics of the interface.[4] Surfactant-coated droplets appear more deformable than protein-coated droplets.[5] Rather than the equilibrium interfacial tension, this work also showed that interfacial *rheology* is the principal governor of the dynamic deformation process. The present study further investigates this phenomenon by using an atomic force microscope (AFM) to quantify the shape relaxation of deformed droplets to an equilibrium state. A controlled dynamic shape perturbation is achieved by driving a droplet pair together at constant velocity, forming a non-equilibrium TLF subject to hydrodynamic and surface forces. The relaxation process was monitored directly by freezing the feedback-loop of the AFM at a prescribed time instant to arrest the applied drive. By adsorbing various components to the oil–water interfaces, the effect of interface structure upon droplet–droplet interactions and TLF relaxation dynamics can be investigated. In thin film experiments, which studied the drainage behaviour of water from between two approaching surfaces, the nature and physical properties of the interfacial species has been shown to determine drainage rates.[6–8] Important factors include the physical size and chemical characteristics of the interfacial species, the level of interactions and their mobility on the interface.

Experimental methods for creating microscopic TLFs can be usefully classified into two groups; supported films and directed particles.[9,10] Supported films are arranged on frameworks or formed into capillaries. The cells developed by Scheludko[11] and Mysels[12] are venerable examples. Early work of Platikanov[13] formed wetting films by expressing a bubble from a capillary against a flat solid surface to garner evidence for the characteristic dimple evolution of TLFs. Alternatively, a microscopic

Institute of Food Research, Norwich Research Park, Colney, Norwich NR4 7UA, UK. E-mail: patrick.gunning@ifr.ac.uk; Fax: +44 1603 507723; Tel: +44 1603 255201

TLF can be also formed by manoeuvring a particle (bubble, droplet or solid sphere) to approach another interface: either a bulk substrate or a second particle. Gravity or buoyancy forces have often been harnessed[14,15] to drive the 'projectile' particle against the target. More recently, the AFM has been used to provide intimate control over approach speed or impact force.[16–18] From the beginning, the mathematical analysis of TLF drainage has exploited the scale disparity parallel and perpendicular to the bounding interfaces (that is, the film 'thinness') in order to make analytic progress: so-called lubrication theory. For the close approach of two droplets, the geometric assumption of a uniform planar film was soon found inadequate, however, initially leading to various ad-hoc treatments of the dimpling effect[19–21] and later more rigorous theories[22–24] that self-consistently evaluate the interface deformation and account for surfactant transport. It has now become clear that TLF drainage in soft matter is determined by a subtle interplay of hydrodynamics, geometric deformation and surface forces.[25] Extensive AFM studies on TLFs carried out over the past decade[26–28] have culminated in the development of a mathematical model that successfully describes inter-droplet force behaviour[29,30] for a generic class of emulsion systems. Factors studied include the effects of droplet velocity,[31] continuous phase viscosity,[32] interfacial charge,[33] and the consequences of absorbing or non-adsorbing polymers[34] present in the continuous phase which give rise to structural forces.[34,35] One aspect not accounted for in the model is the possible role of interfacial rheology in dynamically modulating inter-droplet forces. Intriguingly, the analysis[29,30] accurately reproduces the force interactions for surfactant coated and uncoated droplets using a boundary condition appropriate for an immobile interface that precludes momentum transfer between the bulk phases. The distinction between this no-slip boundary and a stress-free condition describing a mobile interface only has a small quantitative effect on the calculated force–distance relationship without altering the qualitative behaviour.[36] However, classical colloid theory suggests that for liquid–liquid systems, such as surfactant-stabilised emulsion droplets, interfacial rheology should play an important role in mediating inter-droplet interaction.[37] To address this apparent anomaly, and to shed light upon the consequences of interfacial rheology for the forces between colliding oil droplets this study presents an experimental method, capable of resolving behavioural differences for droplets differing markedly in non-equilibrium interfacial response.

Experimental

The oil used in the present study was *n*-tetradecane. Excess surface active impurities were removed by running the oil sequentially through two Florisil® columns (Sigma-Aldrich, St Louis. MA, USA). The interfacial tension was determined to be 54 mN m^{-1}. Fresh solutions of β-lactoglobulin (Sigma L-0130, Lot 078K7430, Sigma Chemicals, Dorset, UK) at 108 μM, β-casein (Sigma C-6905, Lot 30K7442) at 42 μM or Tween-20 (Surfactamps-20, #28320, Lot 1H111031, Thermo Scientific, IL, USA) at 100 μM in water were prepared daily.

Interfacial tension and dilatational rheology measurements

Interfacial tension was measured using the pendant drop technique with a FTA200 pulsating drop tensiometer (First Ten Angstroms, Portsmouth, VA, USA). The appropriate solution of protein or surfactant was placed in a glass cuvette. A Hamilton syringe, having a volume of 25 or 50 μl depending on the droplet size required, was fitted with a j-shaped needle. In the absence of any droplet deformation, interfacial tension was measured over 30 minutes for SDS solutions and 45 minutes for solutions containing Tween 20 or protein. For experiments with salt, sodium chloride was added to the bulk solution containing an existing droplet, and left for several minutes before commencing with the measurement. After equilibration of the interfacial tension, the droplet dilatational response was measured by capturing an image every second for 10 minutes. The computer-controlled dosing system allows triangular time-dependent area deformations to the interface, whilst recording the response of the interfacial tension to the area deformation. The applied interfacial area oscillations were maintained at an amplitude value of 5% and the measurement frequency was 0.1 Hz. The subsequent data is analysed by selecting typically, the 10^{th}–601^{st} collected images. This range is further divided into 10 intervals, each containing approximately 60 images, and a Fast Fourier Transformation (FFT) is applied to each interval. The program then determines the dilatational parameters of the system as a function of the interfacial tension. The dilatational modulus (E) is a complex modulus but, at this frequency, and at the concentrations of protein and surfactant used for the purpose of this study, the viscous component of the dilatational modulus will be very small and the adsorbed layer will be predominantly elastic. All measurements were carried out in triplicate.

Atomic force microscopy

The atomic force microscope used in this study was an MFP-3D-BIO (Asylum Research, Golleta, CA, USA), used with V-shaped silicon nitride cantilevers, 200 μm in length (model NP, Veeco Instruments, Santa Barbara, CA, USA). The spring constant, k, of each lever was calculated in air prior to the addition of droplets using the thermal tune method integrated within the instrument's software. Typical values obtained for k were in the range 0.04–0.08 Nm^{-1}. The attachment of oil droplets to glass slides and to the end of AFM cantilevers has been described in detail previously.[4] Force *versus* distance data for droplet–droplet interactions were obtained by positioning the cantilever-droplet assembly directly over another droplet of approximately equal size (typical radius: 25 μm) that was attached to the glass slide. Each measurement consisted of a force *versus* distance cycle, in which the droplets (initially separated) were first pushed together, and then pulled apart. All data was obtained using the microscope in 'closed-loop' mode to ensure optimal accuracy of the piezo scanner. All relaxation data were captured, by stopping the approach phase of the force–distance cycle at a defined force of 6.4 nN unless otherwise stated, and then monitoring the cantilever deflection over a fixed dwell time. During this dwell period, the AFM held the z stage of the piezoelectric

scanner at a constant position using a secondary feedback loop to eliminate any piezoelectric creep. The duration of this dwell period was typically set at 3 seconds, and the cantilever deflection signal at the photodiode was recorded at a rate of 2 kHz. After the dwell period, the retraction part of the force *versus* distance cycle commenced, and the droplets were separated. Thus, in addition to any relaxation phenomena, the entire force *versus* distance behaviour of the droplets was also recorded in each measurement cycle. All of the data presented were obtained at a scanner velocity of 10 μm s^{-1}. We found these conditions to be optimal to capture relaxation data for the present system.

Interfacial protein films were formed on the droplets by adding appropriate quantities of the protein solution to the water in the liquid cell of the AFM, in order to produce bulk concentrations of 4 μM β-lactoglobulin or β-casein. *In situ* exchange of the interfacial protein film on the droplets was achieved by adding stock Tween-20 solution in order to produce a concentration of 18 μM in the liquid cell, using a methodology similar to that described elsewhere.[5] The protein concentrations were chosen so as to produce a saturated interfacial protein film on the droplets. The surfactant concentration was chosen to ensure complete displacement of the protein from the interface. Following addition of the protein or surfactant a period of 30 minutes allowed the interfacial tension to equilibrate during molecular self-assembly/reassembly at the oil–water interface. Electrolyte concentration was manipulated by adding an appropriate quantity of 100 mM NaCl solution to produce a final concentration of 10 mM NaCl in the liquid cell. A period of at least ten minutes was allowed, following this addition, to ensure adequate mixing of the electrolyte. Sodium dodecyl sulphate (SDS), (Sigma Chemicals, Poole, Dorset UK) was dissolved at a stock concentration of 120 mM, and appropriate aliquots added to the liquid cell of the AFM, in order to produce final SDS concentrations of 6.4 mM.

Results

Fig. 1 illustrates the various stages of the experimental measurement cycle. The changes in cantilever deflection have been converted into force values and plotted as force *versus* distance curves. Fig. 1a shows the force *versus* distance behaviour for a pair of β-lactoglobulin-coated tetradecane droplets being squeezed together. The droplet deformation seen in the approach curve and the hydrodynamic adhesion seen in the retract curves have been reported previously.[4,26] However, upon introducing a dwell period in the force–distance cycle, a new feature emerges in the data; a small offset in the path of the approach (black) and retract (grey) curves. This arises from the relaxation of the cantilever-droplet system that occurs during the dwell period.

Fig. 1b shows the force data plotted as a function of time rather than distance, allowing a clearer appreciation of the relaxation data (red curve in the grey shaded region). Although the extent of relaxation seen in Fig. 1b is small compared to the deflection due to the compression of the droplets during the driven parts of the force–distance cycle (yellow shading),

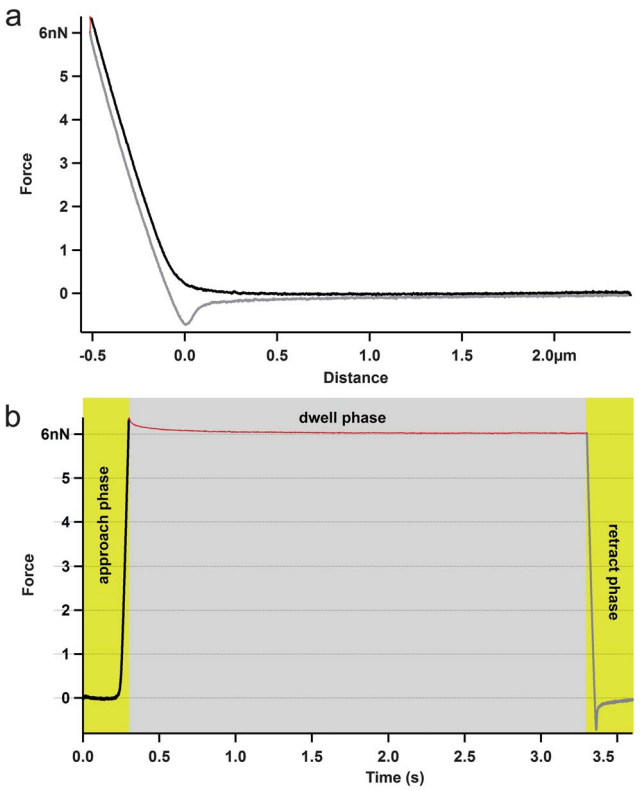

Fig. 1 β-Lactoglobulin-coated oil droplet interaction data plotted as (a) a force *versus* distance curve and (b) a force *versus* time curve, with shading illustrating the different stages of the measurement cycle (yellow – approach and retract, grey – dwell). Relaxation data captured during the dwell phase are shown in red.

examination of this aspect of the data in isolation reveals interesting differences that appear to depend upon the nature of the interfacial film present on the droplets. Fig. 2 shows comparative relaxation data for pairs of droplets coated with SDS, Tween-20 and the globular protein β-lactoglobulin.

It is well known that the surfactants studied here form highly mobile interfacial films[6,38] whilst most surface-active, globular proteins form immobile and elastic interfacial films.[6] Globular proteins such as β-lactoglobulin form interconnected elastic networks at interfaces,[39,40] which possess significantly larger interfacial rheological parameters when compared to

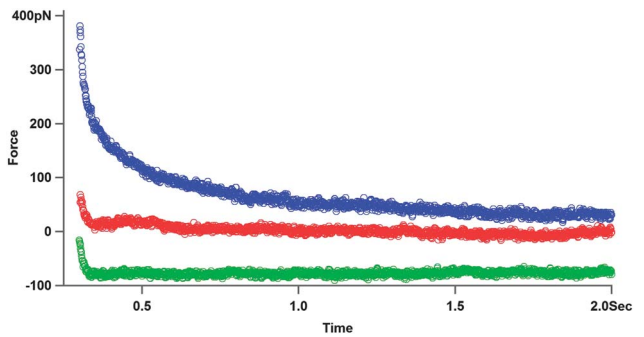

Fig. 2 The effect of the nature of the interface on relaxation data for tetradecane droplets. (Blue) β-lactoglobulin, (red) SDS, (green) Tween-20. Arbitrary vertical offsets have been added to each data set to eliminate overlap.

Table 1 Interfacial characteristics

Droplet interface	Interfacial tension (mN m^{-1})	Dilatational elastic modulus, E (mN m^{-1})
β-Lactoglobulin	24.5 ± 0.6	53.0 ± 0.5
β-Lactoglobulin in 10 mM NaCl	23.5 ± 0.8	50.2 ± 0.6
Tween-20	7.0 ± 0.4	29.8 ± 2.9
Sodium dodecyl sulphate	8.2 ± 0.2	10.2 ± 0.4
β-Casein	17.5 ± 0.7	18.1 ± 0.7

surfactants (Table 1). The protein β-casein by contrast is a rather unique case; although strongly surface-active it forms weakly elastic interfaces[41] (Table 1) due to its lack of secondary structure, and consequently forms interfaces, which exhibit surfactant-like behaviour.[40,42,43] It has been demonstrated previously using AFM force spectroscopy that droplet deformation is affected by the nature of the interfacial film, with β-lactoglobulin-coated droplets appearing less deformable than surfactant (Tween-20) coated droplets.[4] Independent studies using different techniques have confirmed that β-lactoglobulin makes similarly sized oil droplets to the ones used in the present study harder to deform, whilst β-casein coated droplets are easier to deform, confirming the behaviour of the latter is more akin to a surfactant-stabilised system than a protein-stabilised system.[44] This also agrees well with previous work, which demonstrated the importance of shear forces on the interfacial behaviour of proteins.[40] They showed that when a β-casein adsorbed layer was subjected to shear deformation, the response was distinctly fluid-like, similar to a surfactant, particularly at low frequencies, whereas the response of a globular protein, in this case lysozyme, was primarily elastic. This suggests that shear forces could also be important in determining the drainage response between the approaching droplets.

Fig. 3 shows relaxation data observed for uncoated droplets and β-casein coated droplets. The relaxation characteristics in both cases are similar to those seen for the surfactant-coated droplets in Fig. 2. However, there is a notable difference between the β-casein droplet relaxation data and that seen for the uncoated droplets and for droplets coated with surfactants: the magnitude of the relaxation is much larger. The predominant molecular conformation for adsorbed β-casein on a single surface is a long tail at the N-terminus extending far into the aqueous solution.[45] Furthermore, the interaction potential between β-casein layers is predicted to be strongly repulsive at all ionic strengths, which is consistent with the good combined steric and electrostatic stabilisation of β-casein-coated emulsion droplets.[43,45] The larger relaxation magnitude seen for the β-casein coated droplets in the AFM data in Fig. 3 most likely reflects this increased interaction range.

Having touched upon the relative magnitudes of the relaxation data in Fig. 2 and 3 one obvious limitation with this technique is that the absolute droplet separation cannot be measured directly in these experiments. However, by manipulating the ionic strength of the bulk phase (in this experiment the bathing solution) it becomes possible to exert some control over the final thickness of the TLFs that form between approaching droplets. If the experiment is carried out in pure water the screening of the electrostatic charges present on the droplets will be very low (or even entirely absent), and the double layers associated with each droplet will overlap at relatively large separation distances, causing repulsion at large separations. Due to their deformability, the distance of closest approach for droplet surfaces is controlled by the magnitude of the repulsive disjoining pressure.[29] Conventionally when the disjoining pressure equals the Laplace pressure inside the

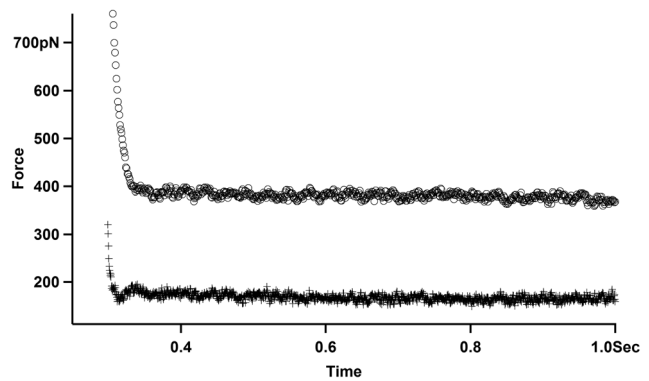

Fig. 3 Relaxation data for; (+) uncoated tetradecane droplets and (○) β-casein coated droplets. Arbitrary vertical offsets have been added to each data set to eliminate overlap. Trigger force 800 pN.

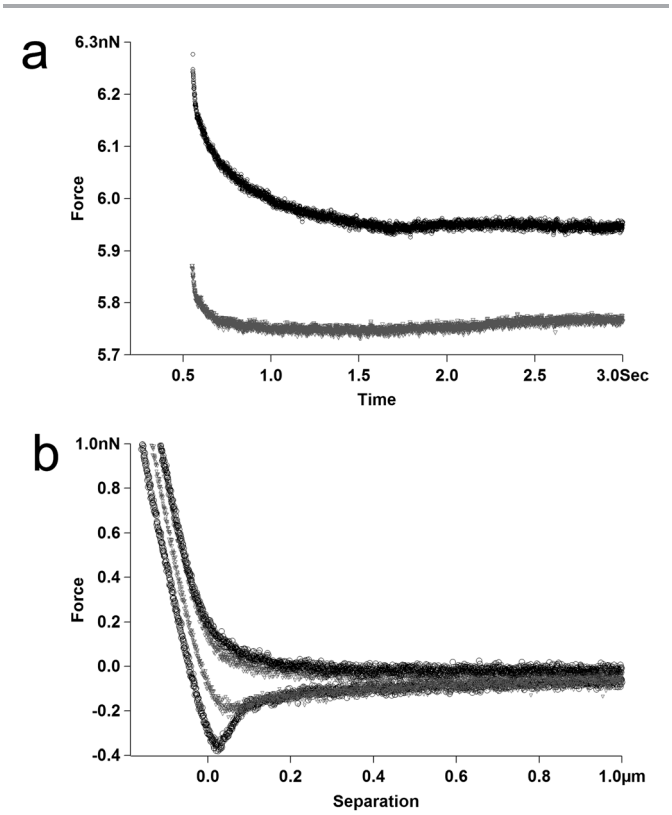

Fig. 4 Effect of bulk phase ionic strength on β-lactoglobulin-coated droplets: pure water (grey) or 10 mM NaCl (black). (a) Relaxation data – with arbitrary vertical offsets to eliminate overlap. (b) Force–distance data.

droplets they will begin to form a flattened face that will grow radially as they approach one another, limiting the extent of thinning of the TLF. If electrolyte is added to the bulk phase, the double layers are shortened, allowing the droplet surfaces to get closer together before they 'feel' any electrostatic repulsion, leading to the formation of a much thinner TLF between the droplets. Fig. 4a shows relaxation curves obtained for a pair of β-lactoglobulin-coated droplets in pure water, and the data obtained for the same droplets following the addition of 10 mM NaCl to the liquid cell. The data clearly illustrates that the increase in ionic strength correlates with a larger magnitude relaxation curve with a slower rate.

In order to probe what prompts this change in relaxation behaviour the complimentary force *versus* distance data obtained in the measurement is presented in Fig. 4b. The gradient of the force *versus* distance data in the constant compliance region of the curves has been shown to correspond with the deformability of the droplets.[4] Examination of the gradient in this region of the data presented in Fig. 4b reveals that the addition of salt to the system has a negligible effect on the apparent deformability of the protein-coated droplets.

Discussion

Together, the relaxation and force *versus* distance data strongly indicate that hydrodynamic drainage of the TLF is the principal origin of the relaxation phenomena observed in the AFM data. The drainage characteristics and surface lateral diffusion properties of TLFs in foam lamellae have been studied previously using the 'thin-film apparatus' and fluorescence recovery after photobleaching (FRAP) for protein-stabilised and surfactant-stabilised foams.[8,46] Tween-20 was shown to form highly mobile interfaces that exhibited fast TLF drainage properties.[6] By contrast, the protein β-lactoglobulin was shown to form immobile interfaces with significant rheology, and TLF drainage was slow at both the air–water and oil–water interfaces.[47] Thus, material transport within the interfacial film was shown to have a profound effect upon TLF drainage. Previous mathematical analysis has shown that the elasticity of the adsorbed surfactant layer plays a key role in the thinning rate and stability of the TLFs between emulsion droplets.[48,49] The data obtained from uncoated-droplets, surfactant-coated droplets and β-casein-coated droplets all exhibit relatively fast relaxation (Fig. 2 and 3). For the surfactant-coated droplets this is presumably dependent on the mobile nature of the interfacial films. Additionally, in the case of β-casein, the fast relaxation observed (Fig. 3) is most likely due to the relatively rapid flow of the weak protein network under the applied stress.[42] Indeed, previous studies have demonstrated that TLFs stabilised by β-casein exhibit classical Derjaguin–Landau–Verwey–Overbeek (DLVO) behaviour,[43] as did Tween-20 stabilised films. The interfacial tension will, of course, vary for each type of interface, as detailed in Table 1. Whilst this variation can clearly influence and give rise to the subtle differences seen in the relaxation data obtained on the surfactant-coated droplets, the data in Fig. 4 show that it is unlikely to be the principal determinant of the slower relaxation seen for droplets coated with β-lactoglobulin, since the addition of salt causes a significant change in relaxation, yet only a negligible change in interfacial tension or elasticity (Table 1).

Comparison of the interfacial elasticity of the droplets reveals that β-lactoglobulin-coated droplets exhibit significantly higher values than all of the other systems studied (Table 1). This suggests a correlation between higher interfacial elasticity and slower relaxation. The data for the β-lactoglobulin-coated droplets appears rather similar to the creep behaviour of a viscoelastic material yielding[50] under load. Thus a possible explanation for the observed relaxation behaviour seen for β-lactoglobulin-coated droplets might be energy dissipation and rearrangement of the protein network at the interface under load. It has previously been suggested that β-lactoglobulin-stabilised emulsion droplets actually behave more like discrete 'capsules' rather than liquid droplets.[44] This may imply that the droplets continue to deform during the dwell period. However, the more pronounced nature of the relaxation seen upon addition of salt (Fig. 4a) cannot be explained by creep since this has no significant effect on the dilatational elasticity of the β-lactoglobulin-coated droplets. The most significant change when the ionic strength has been raised is the increased depth of the minimum seen upon retraction of the droplets in the force *versus* distance data in Fig. 4b. Previous studies have noted that at higher ionic strength, where the Debye length is shorter, a deeper attractive minimum occurs upon retraction of droplets due to the resultant thinner TLF restricting the hydrodynamic drainage.[29] The deeper minimum seen in Fig. 4b following the addition of salt therefore confirms that the TLF between the droplets has become thinner. Thin film studies have already demonstrated that drainage is slower for protein-coated interfaces than for surfactant-coated interfaces,[6,43,47] which is due to the interfacial mobility of the surfactant interface enhancing the drainage rate of interlamellar fluid. This strongly suggests that the relaxation behaviour observed in this study is principally determined by the rate of thin film drainage.

Although mobile interfaces can enhance TLF drainage, the Marangoni effect can also theoretically act to resist TLF drainage through the stress applied to the continuous phase by diffusing surfactant. As liquid drains from the film, a surface tension gradient may be set up radiating from the centre of the film, which would promote diffusion of surfactant back into the centre of the film. In this scenario diffusion of the surfactant would drag interlamellar fluid back into the centre of the film, and hence slow drainage. Furthermore, since the head groups of the surfactants studied (Tween-20 and SDS) are very different in size this should affect their interaction with the aqueous phase, and so if the Marangoni effect were significant in the present study, one would expect to observe differences in drainage rate between the SDS and the Tween-20. There are small differences in the observed relaxation rates of Tween-20 and SDS coated droplets, with the latter exhibiting slightly slower relaxation, but these are not significant in terms of the measurement variability. Therefore in the present study we can conclude that the Marangoni effect is not having a significant influence on the liquid drainage from the film by comparison to that of the interfacial elasticity.

Let us consider how interfacial elasticity influences TLF drainage. There are two factors at play, and each will combine to drive the major differences seen for the relaxation data of β-lactoglobulin-coated droplets compared to the other cases presented in this study. Firstly, previous AFM observations have shown that for droplets in this size range, increased interfacial elasticity makes the droplets less deformable[4] so that when forced together, β-lactoglobulin-coated droplets will therefore be more effective at squeezing out the intervening TLF. As the TLF becomes thinner the increased geometrical confinement from the approaching droplets means that the nature of the interfacial layer will influence hydrodynamic drainage to a greater extent. This bring us to the second factor; the increased interfacial elasticity of the β-lactoglobulin network on the droplets, which the water has to push through, will act to impede the drainage of the TLF in contrast to a mobile interfacial layer (*e.g.* surfactants). Thus the data presented in this study demonstrates that in protein-stabilised emulsions it is the shear resistance of the interfacial protein network which determines the drainage properties on the system scale. This hypothesis is consistent with previous observations in thin film studies; it has been shown that interaction between the β-lactoglobulin layers appear DLVO-like at large distances, while at short distances the overlap of adsorbed protein layers transforms the interaction into a steric-like steep repulsion.[43]

In the unique case of uncoated droplets the fast and limited relaxation observed in Fig. 3 is most likely attributable to droplet flattening at large separation due to long-range electrostatic repulsion, since the droplets bear significant charge in pure water. To attribute this to interfacial mobility or lack of rheological characteristics is not possible because these parameters are more or less impossible to properly determine in the case of an uncoated interface. Unfortunately it was not possible to carry out the charge screening experiment on the uncoated droplet system, as once the ionic strength was raised by the addition of salt the uncoated droplets coalesced when brought together.

Recent modelling studies predict dimple formation in oil droplets in the early stages of retraction.[31] Furthermore, reversal of radial flow direction during TLF drainage involving deformable fluid drops has long been predicted.[50] Thus the available evidence suggests that the thickness of the aqueous film, trapped between colliding oil droplets, is a dynamic quantity during the dwell time between the approach and retract phases of the force–distance cycle in AFM measurements. Irrespective of whether dimple formation occurs in the present case, it seems reasonable to assume that some drainage may continue to occur from between the droplets after the approach cycle has been stopped (*i.e.* during the dwell period).[51,52] The experimental relaxation data presented here provide direct evidence that this is, in fact, the case. The composition and structure of the interfacial film has been shown to affect the measurements significantly, and consequently supports the hypothesis that the experimental relaxation measurements presented here can enhance and contribute to the detailed study of the effects of interfacial structure and rheology on emulsion droplet interactions.

Conclusions

The present studies suggest that AFM relaxation measurements can be used to probe non-equilibrium behaviour for interacting oil droplets and the effects of interfacial structure on TLF drainage, providing an experimental method for probing interactions between soft colloids in more detail. By incorporation into mathematical models this approach may lead to new methods for rational improvement in the functionality of foams and emulsions. For systems such as food emulsions the continuous phase is always complex containing a range of species including, for example salts, sugars, polymers and/or surfactants, all of which affect the nature of the droplet interactions. Understanding and manipulating the interfacial structures to modify the hydrodynamic drainage may provide new opportunities for controlling the stability of these systems.

Abbreviations

AFM	Atomic force microscopy
TLF	Thin liquid film
FFT	Fast Fourier transform
SDS	Sodium dodecyl sulphate
FRAP	Fluorescence recovery after photobleaching.

Acknowledgements

Funding for this work was provided by BBSRC through its core strategic grant to IFR.

References

1 D. Y. C. Chan, E. Klaseboer and R. Manica, *Soft Matter*, 2011, **7**, 2235–2264.
2 E. D. Manev and A. V. Nguyen, *Int. J. Miner. Process.*, 2005, **77**, 1–45.
3 A. Oron, S. H. Davis and S. G. Bankoff, *Rev. Mod. Phys.*, 1997, **69**, 931–980.
4 A. P. Gunning, A. R. Mackie, P. J. Wilde and V. J. Morris, *Langmuir*, 2004, **20**, 116–122.
5 N. C. Woodward, A. P. Gunning, J. Maldonado-Valderrama, P. J. Wilde and V. J. Morris, *Langmuir*, 2010, **26**, 12560–12566.
6 M. Coke, P. J. Wilde, E. J. Russell and D. C. Clark, *J. Colloid Interface Sci.*, 1990, **138**, 489–504.
7 D. C. Clark, P. J. Wilde and D. R. Wilson, *J. Inst. Brew.*, 1991, **97**, 169–172.
8 P. Wilde, A. Mackie, F. Husband, P. Gunning and V. Morris, *Adv. Colloid Interface Sci.*, 2004, **108**, 63–71.
9 A. Sheludko, *Adv. Colloid Interface Sci.*, 1967, **1**, 391–464.
10 I. B. Ivanov and D. S. Dimitrov, in *Thin Liquid Films*, ed. I.B. Ivanov, Marcel Dekker, New York, 1988.
11 A. Sheludko, *Kolloid-Z.*, 1957, **155**, 39–44.
12 K. J. Mysels, *J. Phys. Chem.*, 1964, **68**, 3441–3448.
13 D. Platikanov, *J. Phys. Chem.*, 1964, **68**, 3619–3624.
14 S. Hartland, *J. Colloid Interface Sci.*, 1968, **26**, 383–394.

15 K. A. Burrill and D. R. Woods, *J. Colloid Interface Sci.*, 1973, **42**, 15–34.
16 V. S. J. Craig, C. Neto and D. R. M. Williams, *Phys. Rev. Lett.*, 2001, **87**, 054504.
17 E. Bonaccurso, H.-J. Butt and V. S. J. Craig, *Phys. Rev. Lett.*, 2003, **90**, 144501.
18 E. Bonaccurso, M. Kappl and H.-J. Butt, *Curr. Opin. Colloid Interface Sci.*, 2008, **13**, 107–119.
19 S. P. Frankel and K. J. Mysels, *J. Phys. Chem.*, 1962, **66**, 190–191.
20 K. A. Burrill and D. R. Woods, *J. Colloid Interface Sci.*, 1969, **30**, 511–524.
21 S. Hartland and J. D. Robinson, *J. Colloid Interface Sci.*, 1977, **60**, 72–81.
22 J.-D. Chen, *J. Colloid Interface Sci.*, 1985, **107**, 209–220.
23 S. G. Yiantsios and R. H. Davis, *J. Colloid Interface Sci.*, 1991, **144**, 412–433.
24 L. Y. Yeo, O. K. Matar, E. Susana Perez de Ortiz and G. F. Hewitt, *J. Colloid Interface Sci.*, 2003, **257**, 93–107.
25 D. Y. C. Chan, E. Klaseboer and R. Manica, *Soft Matter*, 2009, **5**, 2858–2861.
26 R. R. Dagastine, G. W. Stevens, D. Y. C. Chan and F. Grieser, *J. Colloid Interface Sci.*, 2004, **273**, 339–342.
27 R. R. Dagastine, R. Manica, S. L. Carnie, D. Y. C. Chan, G. W. Stevens and F. Grieser, *Science*, 2006, **313**, 210–213.
28 H. L. Lockie, R. Manica, G. W. Stevens, F. Grieser, D. Y. C. Chan and R. R. Dagastine, *Langmuir*, 2011, **27**, 2676–2685.
29 S. L. Carnie, D. Y. C. Chan, C. Lewis, R. Manica and R. R. Dagastine, *Langmuir*, 2005, **21**, 2912–2922.
30 D. Y. C. Chan, E. Klaseboer and R. Manica, *Adv. Colloid Interface Sci.*, 2011, **165**, 70–90.
31 G. B. Webber, S. A. Edwards, G. W. Stevens, F. Grieser, R. R. Dagastine and D. Y. C. Chan, *Soft Matter*, 2008, **4**, 1270–1278.
32 R. R. Dagastine, G. B. Webber, R. Manica, G. W. Stevens, F. Grieser and D. Y. C. Chan, *Langmuir*, 2010, **26**, 11921–11927.
33 L. Y. Clasohm, I. U. Vakarelski, R. R. Dagastine, D. Y. C. Chan, G. W. Stevens and F. Grieser, *Langmuir*, 2007, **23**, 9335–9340.
34 A. Gromer, R. Penfold, A. P. Gunning, A. R. Kirby and V. J. Morris, *Soft Matter*, 2010, **6**, 3957–3969.
35 R. F. Tabor, D. Y. C. Chan, F. Grieser and R. R. Dagastine, *J. Phys. Chem. Lett.*, 2011, **2**, 434–437.
36 S. A. Edwards, S. Carnie, O. Manor and D. Y. C. Chan, *Langmuir*, 2009, **25**, 3352–3355.
37 D. A. Edwards, H. Brenner and D. T. Wasan, in *Interfacial Transport Processes and Rheology*, Butterworth-Heinemann, Stonheam, 1991.
38 D. C. Clark, R. Dann, A. R. Mackie, J. Mingins, A. C. Pinder, P. W. Purdy, E. J. Russell, L. J. Smith and D. R. Wilson, *J. Colloid Interface Sci.*, 1990, **138**, 195–206.
39 J. Kragel, R. Wustneck, F. Husband, P. J. Wilde, A. V. Makievski, D. O. Grigoriev and J. B. Li, *Colloids Surf., B*, 1999, **12**, 399–407.
40 E. M. Freer, K. S. Yim, G. G. Fuller and C. J. Radke, *Langmuir*, 2004, **20**, 10159–10167.
41 M. J. Ridout, A. R. Mackie and P. J. Wilde, *J. Agric. Food Chem.*, 2004, **52**, 3930–3937.
42 A. R. Mackie, A. P. Gunning, P. J. Wilde and V. J. Morris, *J. Colloid Interface Sci.*, 1999, **210**, 157–166.
43 T. D. Dimitrova, F. Leal-Calderon, T. D. Gurkov and B. Campbell, *Langmuir*, 2001, **17**, 8069–8077.
44 P. Fischer and P. Ernie, *Curr. Opin. Colloid Interface Sci.*, 2007, **12**, 196–205.
45 E. Dickinson, *Int. Dairy J.*, 1999, **9**, 305–312.
46 D. C. Clark, A. R. Mackie, P. J. Wilde and D. R. Wilson, *Faraday Discuss.*, 1994, **98**, 253–262.
47 P. J. Wilde and D. C. Clark, *J. Colloid Interface Sci.*, 1993, **155**, 48–54.
48 I. B. Ivanov, *Pure Appl. Chem.*, 1980, **52**, 1241–1262.
49 I. B. Ivanov and D. S. Dimitrov, in *Thin film drainage, in Thin Liquid Films: Fundamentals and Applications*, Marcel Dekker, NY, 1988, pp. 379–496.
50 C. A. Tweedie and K. J. Van Vliet, *J. Mater. Res.*, 2006, **21**, 1576–1589.
51 S. Hartland, *Chem. Eng. Prog., Symp. Ser.*, 1969, **65**, 82–89.
52 I. U. Vakarelski, R. Manica, X. Tang, S. J. O'Shea, G. W. Stevens, F. Grieser, R. R. Dagastine and D. Y. C. Chan, *Proc. Natl. Acad. Sci. U. S. A.*, 2010, **107**, 11177–11182.